Bidirectional development of sprite-producing lightning flashes mapped by the Ebro Lightning Mapping Array

Oscar A. van der Velde[1], Joan Montanyà[1], Serge Soula[2], Nicolau Pineda[3] , Janusz Mlynarczyk[4]

1. Technical University of Catalonia, Lightning Research Group, Electrical Engineering Department, Colom 1, TR1 despatx 056, 08222, Terrassa, Spain
2. Université de Toulouse, Observatoire Midi-Pyrénées, Laboratoire d'Aérologie, Toulouse, France
3. Meteorological Service of Catalonia (SMC), Barcelona, Spain
4. AGH University of Science and Technology, Department of Electronics, Krakow, Poland

ABSTRACT: 32 sprite-producing lightning flashes were recorded in 8 nights in different seasons at the east coast of Spain with a 3D Lightning Mapping Array (LMA), operational since July 2011. The bidirectional development of flashes is analyzed using the time-distance method of *van der Velde and Montanyà* (2013) in order to explain the positioning and timing of the positive cloud-to-ground stroke (+CG) and their consequences for charge removal by the negative leader.

For each event, negative leader extents, altitudes and speeds before and after the +CG stroke, as well as positive leader origins and inferred speeds were summarized. Negative leader speeds exhibited modes at 10^5 and $5 \cdot 10^5$ m s^{-1}. Positive leader speeds ranged between $2 \cdot 10^4$ to $2 \cdot 10^6$ m s^{-1}.

Five examples with different evolutions are discussed: 1) Slow bidirectional development with negative leader termination before the +CG stroke; 2) Fast bidirectional development with the negative leader continuing after the +CG stroke. 3) Slow-fast bidirectional development with a negative leader exhibiting a sudden lowering and speed increase; 4) Fast secondary bidirectional development from a mid-level horizontal positive leader. The negative leader propagated rapidly into the upper positive charge layer, continuing after the +CG stroke; 5) Slow bidirectional development, the negative leader terminated after a long distance (50 km) while the positive leader remained trapped inside negative charge. A +CG stroke subsequently occurred under the cut-off negative leader channel. Carrot sprites tended to be associated with fast extending leaders after the stroke, columniform/mixed sprites with slower side branches.

INTRODUCTION

A lightning flash usually initiates between two regions of opposite charge in a thundercloud and develops bidirectionally, with a positive leader growing into negative charge and a negative leader growing into positive charge layers (e.g. *Kasemir,* 1960; *Mazur and Ruhnke* 1993, 1998; *Mansell et al.* 2002; *Aleksandrov et al.*, 2005; *Riousset et al.*, 2007). Lightning mapping studies have had difficulties directly detecting the positive leader end during a flash, but it is well known that some sources from this end can be detected, usually emitted by recoil processes (retrograde negative leaders), which together with

* Contact information: Oscar van der Velde, Technical University of Catalonia, Terrassa (Barcelona), Spain, Email: oscar.van.der.velde@upc.edu

sources from negative leaders give intracloud flashes a bilevel structure (e.g. *Mazur*, 2002; *Rust et al.*, 2005). These sources appear to move away from the flash origin at speeds around $2 \cdot 10^4$ m s^{-1} (e.g. *Proctor et al.*, 1988; *Shao and Krehbiel* 1996; *van der Velde and Montanyà,* 2013).

Studies of sprite-triggering positive cloud-to-ground flashes (+CG) using data from lightning mapping arrays in the United States (e.g. *Stanley*, 2000; *Lyons et al.*, 2003; *Lu et al.* 2009, 2013; *Lang et al.*, 2010, 2011) focused on the negative leader processes after the +CG return stroke and the corresponding charge moment changes which equate to strong quasi-electrostatic fields in the mesosphere required for triggering a sprite (sprites are reviewed by *Pasko et al.* 2012). The bidirectional evolution of the flashes basically was ignored, while it can explain the timing and distance of a +CG stroke from the point the flash initiated. According to *Kasemir* (1960), the electric potential and the length of the bileader determine how much charge is exchanged during the return stroke. This potential is determined not only by the polarity of the return stroke but also by the opposite charge a leader passed through.

In this paper we examine 5 examples differing in bidirectional leader origins, leader speed and continuation of leaders after the +CG stroke, using data from the Ebro Lightning Mapping Array in eastern Spain.

DATA

The dataset of 32 sprite events includes 8 storms, 4 of which were relatively small, less organized and in colder conditions than US Great Plains storm systems. The Ebro LMA locates leader emissions in three dimensions by time-of-arrival of radio pulses in the VHF 60-66 MHz band, every 80 microseconds. In 2011 6 stations were active (12 by 31 km area), in early 2012 8 stations, and in late 2012 and 2013 11 stations within a area of 40 by 70 km. Processing required 5 or more stations to locate a source. The best data (21 of 32 events) is found within 30 km of the center. The *LINET* (*Betz et al.,* 2004) low frequency time-of-arrival network detected intracloud and cloud to ground pulses. A 2D VHF interferometer of the Meteorological Service of Catalonia provided complementary intracloud lightning data.

Several low-light cameras detected sprites over the Ebro LMA region. They were located at Pic du Midi and Rustrel in southern France and in central Catalonia (100-500 km distance). The images were fitted to star charts to find azimuths and elevations of sprites, while GPS timestamps made comparison with LMA data possible, with interlaced fields lasting 20 ms.

METHODS

The main data analysis uses the time-distance-altitude projection of *van der Velde and Montanyà* (2013) with the point of reference being the +CG stroke (alternatively, the flash initiation point). This projection has the advantage of allowing a time axis along with spatial development in the vertical and one horizontal dimension. This avoids disadvantages of overlapping developments or subtle time-color differences in conventional projections. Reference slopes indicate approximate speeds (10^6, 10^5, $2 \cdot 10^4$ m s^{-1}) which help the identification of leaders in combination with altitude coloring, because charge tends to be layered (e.g. blue sources, weak slope – mid level positive leader, red sources, steeper slope – upper level negative leaders, see examples in *van der Velde and Montanyà*, 2013). For accurate leader speed calculations, determined for all 32 events before and after +CG strokes, the actual distance and elapsed

time were used.

RESULTS

We briefly present 5 alternative examples to those included in *van der Velde et al.* (2014), with similar evolutions. A table of events and their leader properties was also included in that paper. We include here the values just for the examples below. There is a large variation in leader lengths and speed before and after the return stroke.

Table 1. Leader characteristics before and after the +CG return stroke.

E #	Event time SP+CG stroke	Leader [-] before SP+CG stroke			Leader [-] after SP+CG stroke			Leader [+] (inferred)			+CG stroke		Sprite	
	UTC	Dist. km	Alt. km	Speed m s^{-1}	Dist. km	Alt. km	Speed m s^{-1}	Dist. km	Altitude km	Speed m s^{-1}	Timing ms	Peak kA	Delay ms	Type
1	24 Sep 2011 03:26:57.633/661	40 SW	9–6	2E+5	40 ESE	5.5–8	2E+5	3.5	5	4E+4	240	+16 +67	28-48 0-1	not clear
2	3 Apr 2012 20:24:32.607	4 (x2)	4.5 – 6.5	2E+5	15 e 5	5 – 6.5	8E+5	7.5	4.5	5E+5	23	+119	3-23	carrot group
3	20 Nov 2011 03:49:07.074	30	8–6 → 5–3	1E+5 4E+5	<5	5.5–7.5	6E+4	20 13	5.5 4	2E+5 3E+5	135 63	- +122	0-9	column group with carrot
4	20 Nov 2011 03:23:31.894 ?	5	3.5 → 7	4E+5	15 e 5	5.5–7.5	4E+5	4	3.5	9E+5	9	+10	48-68 (23-43)	one column
5	24 Sep 2011 03:29:27.338	48	10--6	1E+5	20	5–7.5	1E+5	12 2	4 6	2E+4 2E+4/3E+5	500 330 or 30	- +24		No sprite detected

In the following discussion and figures the flash initation is marked (0), initial negative leaders (1), initial positive leaders (2), when detected by VHF sources, and negative leader activity after the return stroke by (3) and (4). The remaining leader activity during each flash (>100 ms after the +CG stroke) is not discussed.

Example 1

In this event in Fig. 1 a high altitude negative leader (1) moved 40 km to the southwest from the initiation point at a speed of $2\cdot 10^5$ m s^{-1}. It stopped just before the +CG stroke. The mid level positive leader (2) leading to the first +CG stroke only 3.5 km away from the origin was detected by a few sources from recoil events on the line in the time-distance plot between origin and +CG stroke (at the x-axis) with a horizontal speed of $2\cdot 10^4$ m s^{-1}. In this particular event the first stroke did not trigger a sprite (unlike example 1 in *van der Velde et al.* 2014). Negative leaders developed after this stroke (3) and a second

+CG stroke occurred, followed by 40 km of new negative leader expansion (4), this time to the east-southeast. The sprite was short-delayed to this second stroke.

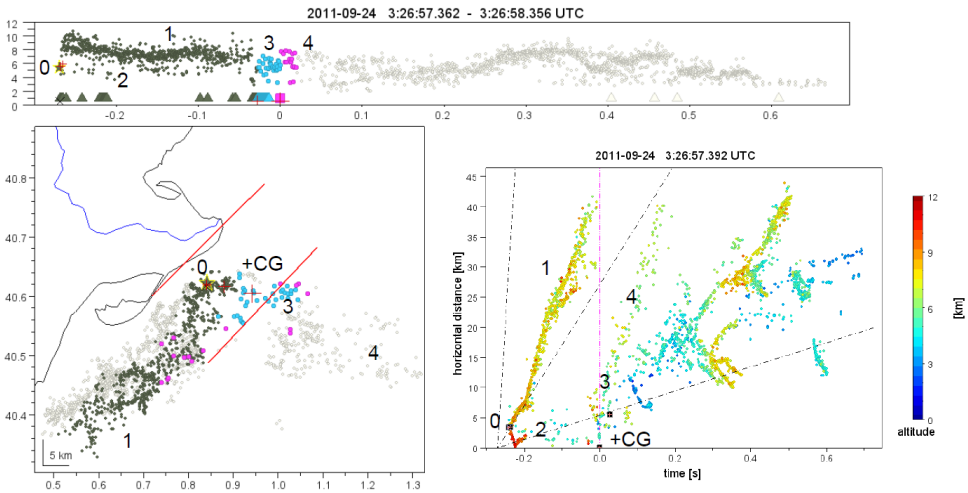

Figure 1. Time-altitude (top), latitude-longitude (left) and time-distance (right) projections for example 1. Approximate sprite range is indicated by red lines. The reference for the time-distance plot was the first +CG stroke.

Example 2

This event (Fig. 2) started with two main negative leader branches (1) propagating from 4.5 km altitude into different directions at about $2\cdot 10^5$ m s^{-1}. The 119 kA +CG return stroke already occurred after 23 ms, 7.5 km away from the initiation point, while negative leaders were still only a few kilometers long. No sources were detected in association with the positive leader. Its inferred speed was $5\cdot 10^5$ m s^{-1}. After the +CG stroke one of the negative leader branches (3) extended at its far end by 15 km at a very high velocity of $8\cdot 10^5$ m s^{-1}. A short-delayed carrot sprite group was triggered during this development.

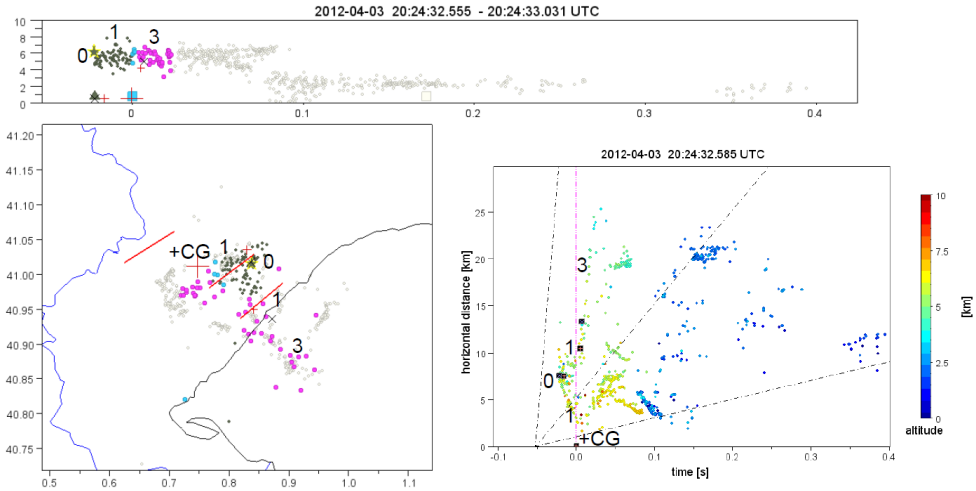

Figure 2. Time-altitude (top), latitude-longitude (left) and time-distance (right) projections for example 2. Approximate sprite element ranges are indicated by red lines. The reference for the time-distance plot was the +CG stroke.

Example 3

Fig. 3 shows an event which at first sight looks similar to example 1. A few negative leaders (1) propagated at $1\cdot 10^5$ m s^{-1} in the upper positive charge region of the convective cell (radar not shown). A few sources associated with recoil events from the positive leader end (2) occurred around 5 km altitude and remained within 1 km from the origin. No +CG stroke follows up on this leader, it terminated in the cloud. Meanwhile, the main negative leader (1) sharply decreased in altitude (from 7 to 4 km), emitting a LF pulse detected by LINET and a series of interferometer sources as it accelerated to $4\cdot 10^5$ m s^{-1}, spreading out into the stratiform region until 30 km distance (3). The +CG stroke triggering the sprite occurred 20 km from the flash origin. It is possible that 1) the negative leader channel somehow initiated a downward positive leader or 2) the point of acceleration marks new bidirectional breakdown with a fast negative and fast positive leader. This will need to be confirmed by optical methods. Post-CG negative leaders (4) involved the convective positive charge.

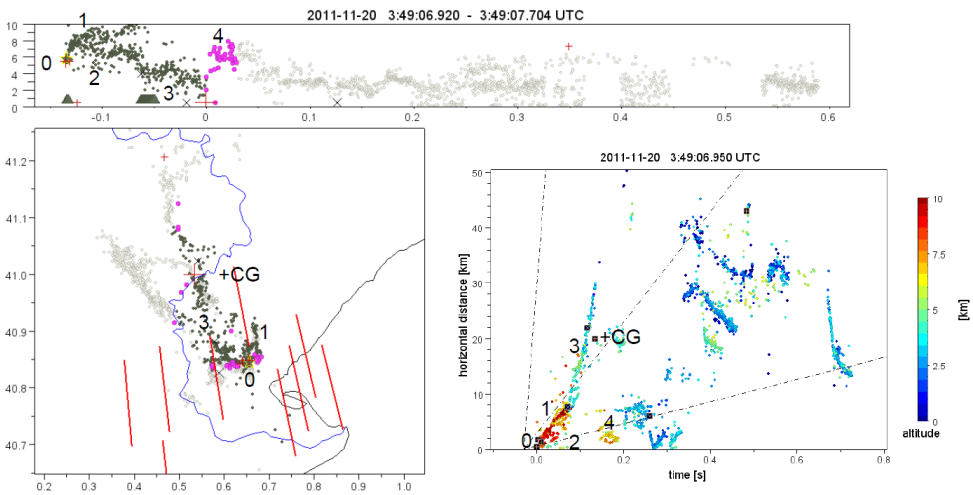

Figure 3. Time-altitude (top), latitude-longitude (left) and time-distance (right) projections for example 3. Approximate sprite range is indicated by red lines. The reference for the time-distance plot was the flash initiation point.

Example 4

This event is displayed in Fig. 4. It started like a -CG flash with some return strokes followed by a period (1) of about 400 ms with slow positive leader propagation ($2\cdot 10^4$ m s^{-1}) at 3 km altitude with sometimes lower altitude negative leaders. Suddenly, from this trace an upward growth of negative leaders took place (3), apparently from a K-event (recoil process), see *van der Velde and Montanyà* (2013), spreading out horizontally at a fast $4\cdot 10^5$ m s^{-1} into higher level positive charge (the time-distance plot shows this as diverging trace). During the initial expansion, several low-frequency pulses were detected in the 6-13 kA range, one of which being the +CG stroke (not clear), as well as a burst of interferometer sources. The negative leaders kept expanding 15 km far after the +CG stroke and a long-delayed single column sprite occurred 48-68 ms after the best +CG stroke candidate detection.

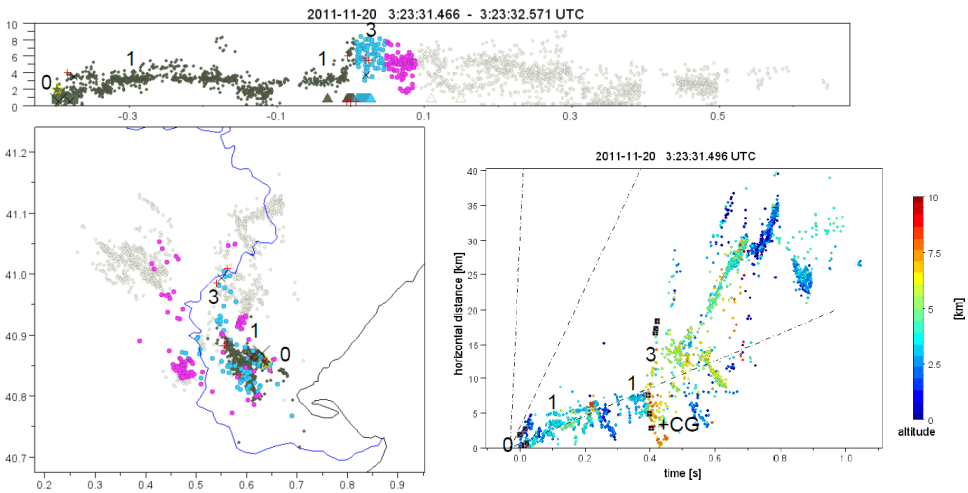

Figure 4. Time-altitude (top), latitude-longitude (left) and time-distance (right) projections for example 4. Approximate sprite range is indicated by red lines. The reference for the time-distance plot was the flash initiation point.

Example 5

In *van der Velde et al.* (2014) we show an example of sprite-producing flash development with slow bidirectional leaders (negative $1\cdot 10^5$ m s^{-1}; positive $2\cdot 10^4$ m s^{-1}) where the positive leader remained trapped inside the negative cloud charge without going to ground, while the negative leader grew more than 50 km long, after which a +CG occurred under that leader, apparently as result of current cut-off.

Here we show a similar flash closer to the Ebro LMA providing more detail. No sprite was detected for this case but sky conditions at the far away camera were not optimal. The time-distance plot shows the negative leader (1) come to the +CG stroke location from its initiation point (0) 35 km away, and reaching a total length of 48 km. Simultaneously at 4 km altitude sources stemming from the positive leader end from the same origin (2) were detected. They indicate several branches. After the negative leader (1) ended, new negative leaders developed again near the origin, while the positive leader (2) terminated without reaching ground (no +CG stroke, in contrast to example 1). However, a +CG stroke was detected under the old negative leader branch some 330 ms after it passed over that location. It was preceded (30 ms earlier) by new negative side branches (3). It is possible that the positive and negative leaders (3) were a result of new bidirectional breakdown along the old, likely cut-off, negative leader (1). These negative leaders continued after the stroke (4).

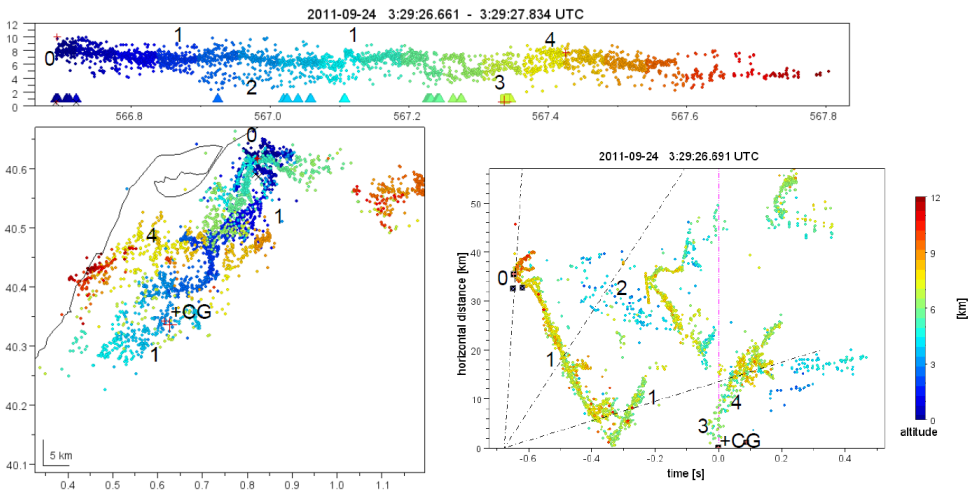

Figure 5. Time-altitude (top), latitude-longitude (left) and time-distance (right) projections for example 5. Approximate sprite range is indicated by red lines. The reference for the time-distance plot was the +CG stroke.

CONCLUSIONS

The 5 examples presented here are a subset of the 32 events summarized by *van der Velde et al.* (2014), where we discussed a similar set of examples. The examples show strong evidence for bidirectional flash development with the +CG at the end of a positive leader opposite to the negative leader, which can be detected when propagating slowly ($2\cdot 10^4$ m s^{-1} horizontally). Fast positive leaders have been inferred from the stroke location and the point of fast negative leader initiation. Example 5 (and possibly example 2) show that a positive leader can initiate from a previous negative leader. Example 4 shows that a negative leader can suddenly emerge from the positive leader trace (escaping recoil/K-leader process) and invade upper positive charge layers – while a weak +CG return stroke indicates a fast positive leader grew to ground at the same time. Reported speeds are in agreement with the wide range observed with optical methods by *Campos et al.* (2013).

Statistics from Table 1 (the 32 events version by *van der Velde et al.* 2014) show that the negative leader speed distribution tended to show two modes. When negative leaders were "fast" (>$3\cdot 10^5$ m s^{-1}) the positive leader also tended to be faster (on average: $4\cdot 10^5$ m s^{-1}). Fast negative leaders also result in intracloud LF pulses (LINET) and VHF interferometer detections as discussed in more detail in that study. When negative leaders were slow, positive leaders tended to be slower as well ($1\cdot 10^5$ m s^{-1}). This suggests the opposite ends are linked to some extent while external factors (e.g. initial and later potential gradients at both ends arising from the charge distribution) control the velocities. Furthermore, the statistics in *van der Velde et al.* (2014) show that initial fast negative leaders tended to keep extending more often at the far end after the +CG stroke (probably because the strokes in those cases tended to occur early, with still limited initial negative leader expansion), which usually corresponded with a charge transfer favorable for carrot sprite morphology (lower altitude clustered forms). Column sprite morphology (the least developed form) was mainly observed in the dataset when negative leaders were slower and had terminated before the +CG return stroke (like examples 1 and 5).

ACKNOWLEDGMENTS

This study was supported by the project AYA2011-29936-C05-04 of the Spanish Ministry of Economy and Competitiveness (MINECO). We thank Oriol Argemí and Txema Media from the Meteorological Service of Catalonia, Xavier Abril from the Delta de l'Ebre Natural Parc, and Germán Solé of Observatori de l'Ebre for hosting our LMA sensors, Martin Füllekrug for his broadband radio data, József Bór for a comparison of charge moment change calculations. David Romero and Robert Rico prepared and installed LMA stations, Gloria Solà and Hans-Dieter Betz supplied *LINET* data. The LMA was built by New Mexico Tech.

REFERENCES

Aleksandrov, N. L., T, E.M. Bazelyan, Yu.P. Raizer (2005), Initiation and development of first lightning leader: The effects of coronae and position of lightning origin. Atmos. Res. 76 (2005) 307–329, doi:10.1016/j.atmosres.2004.11.007

Betz, H.-D., K. Schmidt, P. Oettinger, and M. Wirz (2004), Lightning detection with 3-D discrimination of intracloud and cloud-to-ground discharges, Geophys. Res. Lett., 31, L11108, doi:10.1029/2004GL019821

Campos, L. Z. S. M. M.F. Saba, T. A. Warner, O. Pinto Jr., E. P. Krider, R. E. Orville (2013), High-speed video observations of natural cloud-to-ground lightning leaders – A statistical analysis, Atmos. Res., 135–136, 285-305, doi:10.1016/j.atmosres.2012.12.011.

Kasemir, H. W. (1960), A contribution to the electrostatic theory of a lightning discharge, J. Geophys. Res., 65(7), 1873–1878, doi:10.1029/JZ065i007p01873.

Lang, T. J., W. A. Lyons, S. A. Rutledge, J. D. Meyer, D. R. MacGorman, and S. A. Cummer (2010), Transient luminous events above two mesoscale convective systems: Storm structure and evolution, J. Geophys. Res., 115, A00E22, doi:10.1029/2009JA014500.

Lang, T. J., J. Li, W. A. Lyons, S. A. Cummer, S. A. Rutledge, and D. R. MacGorman (2011), Transient luminous events above two mesoscale convective systems: Charge moment change analysis, J. Geophys. Res., 116, A10306, doi:10.1029/2011JA016758.

Lu, G., S. A. Cummer, J. Li, F. Han, R. J. Blakeslee, and H. J. Christian (2009), Charge transfer and in-cloud structure of large-charge-moment positive lightning strokes in a mesoscale convective system, Geophys. Res. Lett., 36, L15805, doi:10.1029/2009GL038880.

Lu, G., et al. (2013), Coordinated observations of sprites and in-cloud lightning flash structure, J. Geophys. Res. Atmos., 118, 6607–6632, doi:10.1002/jgrd.50459.

Lyons, W. A., E. R. Williams, S. A. Cummer, and M. A. Stanley (2003), Characteristics of sprite-producing positive cloud-to-ground lightning during the 19 July 2000 STEPS mesoscale convective systems, Mon. Weather Rev., 131, 2417.

Mansell, E. R., D. R. MacGorman, C. L. Ziegler, and J. M. Straka (2002), Simulated three-dimensional branched lightning in a numerical thunderstorm model, J. Geophys. Res., 107(D9), doi:10.1029/2000JD000244.

Mazur, V. (2002), Physical processes during development of lightning flashes, Comptes Rendus Phys., 3, 1393–1409.

Mazur, V., and L. H. Ruhnke (1993), Common physical processes in natural and artificially triggered lightning, J. Geophys. Res., 98, 12,913–12,930, doi:10.1029/93JD00626.

Mazur, V., and L. H. Ruhnke (1998), Model of electric charges in thunderstorms and associated lightning, J.

Geophys. Res., 103(D18), 23299–23308, doi:10.1029/98JD02120.

Pasko, V. P., Y. Yair, and C-L. Kuo, (2012), Lightning Related Transient Luminous Events at High Altitude in the Earth's Atmosphere: Phenomenology, Mechanisms and Effects. Space Science Reviews, 168, 1-4, 475-516

Proctor, D., R. Uytenbogaardt, and B. Meredith (1988), VHF radio pictures of lightning flashes to ground, J. Geophys. Res., 93(D10), 12,683–12,727, doi:10.1029/JD093iD10p12683.

Riousset, J. A., V. P. Pasko, P. R. Krehbiel, R. J. Thomas, and W. Rison (2007), Three-dimensional fractal modeling of intracloud lightning discharge in a New Mexico thunderstorm and comparison with lightning mapping observations, J. Geophys. Res., 112, D15203, doi:10.1029/2006JD007621.

Rust, W. D., D. R. MacGorman, E. C. Buning, S. A. Weiss, P. R. Krehbiel, R. J. Thomas, W. Rison, and J. Harlin (2005), Inverted-polarity electrical structures in thunderstorms in the Severe Thunderstorm Electrification Study (STEPS), Atmos. Res., 76, 247–271, doi:10.1016/j.atmosres.2004.11.029.

Shao, X., and P. Krehbiel (1996), The spatial and temporal development of intracloud lightning, J. Geophys. Res., 101(D21), 26,641–26,668, doi:10.1029/96JD01803.

Stanley, M. A. (2000), Sprites and their parent discharges, Ph.D. Dissertation, 163 pp., New Mexico Institute of Mining and Technology, Socorro, NM, USA

van der Velde, O. A. and J. Montanyà (2013), Asymmetries in bidirectional leader development of lightning flashes. J. Geophys. Res., doi: 10.1002/2013JD020257

van der Velde, O. A., J. Montanyà, S. Soula, N. Pineda, and J. Mlynarczyk (2014), Bidirectional origins and speed of positive and negative leaders in sprite-producing +CG flashes J. Geophys. Res., *submitted* (2013JD021291)